available at www.sciencedirect.com

ScienceDirect

journal homepage: www.elsevier.com/locate/biochempharm

Induction of P-glycoprotein expression and function in human intestinal epithelial cells (T84)

I.S. Haslam [a], K. Jones [b], T. Coleman [b], N.L. Simmons [a,*]

[a] Epithelial Research Group, Institute for Cell and Molecular Biosciences, University of Newcastle Upon Tyne, Medical School, Newcastle Upon Tyne NE2 4HH, UK

[b] AstraZeneca, Discovery DMPK, Alderley Park, Macclesfield, Cheshire, UK

ARTICLE INFO

Article history:
Received 18 June 2008
Received in revised form
14 July 2008
Accepted 15 July 2008

Keywords:
Intestine
T84
Pgp
MDR1
Induction

ABSTRACT

Intestinal induction of Pgp is known to limit the oral availability of certain drug compounds and give rise to detrimental drug–drug interactions. We have investigated the induction of P-glycoprotein (Pgp; MDR1) activity in a human intestinal epithelial cell line (T84) following pre-exposure to a panel of drug compounds, reported to be Pgp substrates, inhibitors or inducers.

Human MDR1-transfected MDCKII epithelial monolayers were used to assess Pgp substrate interactions and inhibition of digoxin secretion by the selected drug compounds. The T84 cell line was used to assess induction of Pgp-mediated digoxin secretion following pre-exposure to the same compounds. Changes in gene expression (MDR1, MRP2, PXR and CAR) were determined by quantitative RT-PCR. Net transepithelial digoxin secretion was increased (1.3 fold, $n = 6$, $P < 0.05$) following pre-exposure to the PXR activator hyperforin (100 nM, 72 h), as was MDR1 mRNA expression (3.0 fold, $n = 4$, $P < 0.05$). A number of Pgp substrates (quinidine, amprenavir, irinotecan, topotecan, atorvastatin and erythromycin) induced net digoxin secretion, as did the non-Pgp substrate artemisinin. Various non-Pgp substrates demonstrated inhibition of digoxin secretion (verapamil, mifepristone, clotrimazole, mevastatin, diltiazem and isradipine) but did not induce Pgp-mediated digoxin secretion. Of the compounds that increased Pgp secretion, quinidine, topotecan, atorvastatin and amprenavir pre-exposure also elevated MDR1 mRNA levels, whereas erythromycin, irinotecan and artemisinin displayed no change in transcript levels. This indicates possible post-translational regulation of digoxin secretion. Finally, a strong correlation between drug modulation of MRP2 and PXR mRNA expression levels was evident.

1. Introduction

Members of the ATP-binding cassette (ABC) family of transport proteins such as P-glycoprotein (Pgp, MDR1, ABCB1) can be responsible for limiting the intestinal absorption of a diverse range of xenobiotics [1]. This can result in substantial variability in the oral bioavailability of certain drug compounds. In addition, even in the absence of metabolic interactions, the operation of efflux transporters may lead to a number of potentially detrimental drug–drug, or herb–drug interactions via competition and/or inhibition [1]. This can involve inhibition of the efflux activity by one compound, resulting in the increased absorption of a second drug. Examples of this include altered digoxin absorption following quinidine inhibition [2], increased paclitaxel absorption with cyclosporin A co-administration [3] and mifepristone (RU486) inhibition of various P-glycoprotein substrates [4].

* *Corresponding author*. Tel.: +44 191 2226999.
E-mail address: n.l.simmons@ncl.ac.uk (N.L. Simmons).

0006-2952/$ – see front matter
doi:10.1016/j.bcp.2008.07.020

A novel aspect of the action of P-glycoprotein is seen in examples where drug compounds induce expression of Pgp and so effect the absorption of Pgp substrates without necessarily being substrates themselves. Examples include rifampin co-administered with talinolol [5] and digoxin [6]. In terms of herb–drug interactions, the herbal remedy St. John's Wort contains an active constituent (hyperforin) reported to be responsible for increasing both Pgp and CYP3A4 expression, which has resulted in reduced blood cyclosporine concentrations and transplant rejection in certain cases [7,8].

Induction of ABC transporters, such as Pgp and MRP2 (Multidrug Resistance Related Protein 2, ABCC2), is governed by a number of nuclear hormone receptors, often termed 'xenosensors' for their ability to interact with a broad range of exogenous drugs and toxins [9–12]. In particular, the pregnane X receptor (PXR, NR1I2) and constitutive androstane receptor (CAR, NR1I3) mediate cellular responses to toxic insult by acting as transcription factors for components of the secretory detoxification system, including efflux transporters (Pgp, MRP2) and metabolic enzymes (CYP3A4, 2B6) [9–12]. The ability of a drug compound to interact with a particular nuclear hormone receptor and modulate the expression of effectors is often assessed by reporter-gene assay or transcript induction studies [12,13]. Robust in vitro assays for determining potential changes in functional activity are limited and the relationship between increased gene expression and functional activity is rarely addressed [14]. Both efflux transporters and nuclear receptors display a certain degree of overlap in substrate specificity [15]. Evidence also exists for nuclear receptor cross-talk that may allow for an extra degree of dynamic control and adaptation, not to mention redundancy within the system [15–17]. In this respect, the cellular mechanisms responsible for tailoring the response to xenobiotic exposure reflects a complex network of interacting components.

Recently, we have identified an intestinal cell-line, T84, that co-expresses both P-glycoprotein and PXR that may serve as an appropriate in vitro cell-system for identifying adverse interactions based on induction of P-glycoprotein at the mRNA, protein and functional levels [18]. T84 cells display a similar morphology to undifferentiated crypt cells and form polarised cuboidal epithelial layers when grown on permeable supports [19]. Previous investigations in this laboratory have indicated apical expression of P-glycoprotein [18] and secretion of P-glycoprotein substrates vinblastine and digoxin [18,20]. Importantly the T84 cell-line responds to pre-incubation with rifampin, a specific PXR agonist, by upregulation of Pgp expression and increased secretory transport of the Pgp substrate, digoxin [18]. The purpose of the present investigation was to test a range of drug compounds selected on the basis of MDR1 or PXR interactions, either as substrates, inhibitors or inducing agents, upon induction of functional secretory activity using digoxin as the Pgp substrate, whilst correlating this with modulation of gene transcription (MDR1, MRP2, PXR and CAR). The selected drug compounds were also directly assessed for Pgp substrate or inhibitor activity by the use of transfected MDR1-MDCKII epithelial monolayers. Modulation of transcription was determined using real-time quantitative PCR to assess changes in MDR1, MRP2, PXR and CAR expression levels. Pgp substrates, as defined by transport activity, were most effective as inducers of Pgp activity whereas Pgp inhibitors were usually ineffective. Induction of Pgp-mediated transport in T84 epithelial layers may occur in the presence or absence of increased MDR1 transcription, highlighting the importance of post-transcriptional regulation in Pgp functional activation.

2. Methods

2.1. Materials

[^{14}C]-Mannitol (specific activity 56 mCi mmol^{-1}) and [^{3}H]-digoxin (specific activity 21.8 Ci mmol^{-1}) were from PerkinElmer (Boston, MA, USA). Cell culture media and supplements were from Sigma (Poole, Dorset, UK), and tissue culture plastic flasks and culture plates were supplied by Costar (High Wycombe, UK). Amprenavir was purchased from Moravek Biochemicals (Brea, CA, USA). All other chemicals obtained from Sigma (Poole, Dorset, UK), unless otherwise stated.

2.2. Cell culture

All cell culture was performed in a class II laminar flow hood (Safeflow1.2, Bio Air Instruments, Italy) under aseptic conditions.

MDR1-MDCKII cells are a derivative of wild-type MDCKII cells, stably transfected with the human MDR1 gene, therefore displaying over-expression of P-glycoprotein [21]. Wild-type and transfected cells were maintained in Dulbecco's Modified Eagle's Medium (DMEM) Glutamax (Gibco), supplemented with foetal calf serum (10%, v/v), and glutamine (1%, v/v).

T84 cells were supplied by AstraZeneca (Alderley Park, Cheshire, UK) and used between passage numbers 6–15. Cells were maintained in a 1:1 mix of high glucose (4500 mg ml^{-1}) DMEM and HAMS F12 nutrient mixture, supplemented with foetal calf serum (10%, v/v), HEPES (15 mM) and sodium pyruvate (1 mM). Cells were grown in the presence of an antibiotic mix of penicillin–streptomycin (5%, v/v).

Both T84 and MDR1-MDCKII cells were seeded onto 96-well culture inserts (Transwell 3391, 4.26 mm diameter, 0.4 μm pore size, uncoated polycarbonate filters, Costar) at high density (5×10^5 cells cm^{-2} T84 and 3.6×10^5 cells cm^{-2} MDR1-MDCKII) for use in induction studies. WT- and MDR1-MDCKII cells were seeded into 12-well culture inserts (Transwell 3401, 12 mm diameter, 0.4 μm pore size, uncoated polycarbonate filters, Costar) for digoxin inhibition studies. Cells were maintained at 37 °C in a humidified incubator with 5% CO_2 in air. T84 cells were allowed 7 days and MDR1-MDCKII cells 4 days growth to confluence. T84 cell confluence was determined by measurement of transepithelial electrical resistances (TEER) using a WPI EVOM voltohmeter (World Precision Instruments, Stevenage, Hertfordshire, UK). Resistance values were in excess of 500 Ω cm^2.

2.3. Transepithelial transport experiments

Automated bi-directional transepithelial transport assays were performed using MDR1-MDCKII cells seeded into 96 well transwell transport plates. Transport assays were performed 4

days post-seeding. Transport plates were produced to allow the unidirectional (apical-to-basal, P_{a-b} and basal-to-apical, P_{b-a}) permeability of each compound (10 μM). Sampling was performed using the Tecan RSP 200 Workstation, comprising of the Robotic Manipulator (RoMa) and Liquid Handler (LiHa). Lucifer Yellow (100 μM) was included in the transport buffer to allow post-assay determination of paracellular permeability, measured by spectrofluorometry (485–535). The extent of apical-to-basal and basal-to-apical transport was determined by HPLC-MS/MS sample analysis for each drug compound. Apparent permeability (P_{app}; $\times 10^{-6}$ cm s^{-1}) was calculated for each compound in the apical-to-basal (P_{a-b}) and basal-to-apical (P_{b-a}) directions using the following equation:

$$P_{a-b} = \frac{V_A}{St} \times \frac{D_b}{Dt}$$

$$P_{b-a} = \frac{V_A}{St} \times \frac{D_a}{Dt}$$

where V_A represents the volume in the receiver well, S represents the area of tissue exposed to the solution (1.14 cm^2 or 0.11 cm^2) and t represents time (seconds). D_a and D_b represent the activity (in dpm) transported to the apical and basal receiver, respectively. This allowed for determination of the efflux ratio (P_{b-a}/P_{a-b}) for each compound.

Bi-directional transepithelial transport experiments using the MDR1 substrate digoxin were performed using T84 cells 7–10 days post-seeding. Prior to flux experiments, cells were pre-treated for 72 h with a number of drug compounds; mifepristone, cimetidine (50 μM), verapamil, atorvastatin, isradipine, diltiazem, mevastatin, lovastatin, clotrimazole, erythromycin (50 μM), irinotecan, artemisinin, quinidine, amprenavir, topotecan (1 μM) hyperforin, (100 nM) or the vehicle control, DMSO (0.1%, v/v). All drug compounds were added to both the apical and basolateral compartments. All drug concentration were 10 μM unless otherwise stated. Subsequently, cell monolayers were allowed a 3 h wash period in drug-free medium. Layers were then washed (three times) in Hanks Buffered Saline Solution (HBSS) and placed in a fresh 96 well base-plate containing 200 μl HBSS supplemented with 10 mM HEPES. Monolayers were allowed a 15 min equilibration period at 37 °C prior to TEER recordings. For flux experiments, the buffer composition was identical for apical and basal compartments (HBSS + 10 mM HEPES) with the addition of 0.1 μM [^{3}H]-digoxin and 1 μM [^{14}C]-mannitol to either the apical or basal compartments. Samples were taken to determine absorptive (apical-to-basal, P_{a-b}) and secretory (basal-to-apical, P_{b-a}) permeability following a 1 h incubation at 37 °C. Net secretion (P_{net}) was calculated from paired monolayers by subtracting apical-to-basal (P_{a-b}) from basal-to-apical (P_{b-a}) permeabilities.

Inhibition of bi-directional digoxin flux was determined in wild-type and MDR1-transfected MDCKII cell layers. Cultures were allowed 4 days growth to confluence prior to use. Monolayer integrity was determined by measurement of the bi-ionic dilution potentials, which were typically in the range of 20–30 mV. Cells were equilibrated for 15 min in a Krebs' buffer consisting of 137 mM NaCl, 5.4 mM KCl, 1 mM $MgSO_4$, 0.3 mM NaH_2PO_4, 0.3 mM KH_2PO_4, 10 mM glucose and 10 mM HEPES (buffered to pH 7.4 at 37 °C with Trizma base). Following this layers were pre-incubated (15 min) in Krebs' solutions containing mifepristone, cimetidine (50 μM), verapamil, atorvastatin, isradipine, diltiazem, mevastatin, lovastatin, clotrimazole, erythromycin (50 μM), irinotecan, artemisinin, quinidine, amprenavir, topotecan (1 μM) or the vehicle control, DMSO (0.1%, v/v). All drug concentrations were 10 μM unless otherwise stated. Cell layers were transferred into fresh plates, with the addition of donor transport solutions containing the relevant drug compound (see above) as well as [^{3}H]-digoxin (0.5 μCi mL^{-1} plus 1 μM unlabelled) and [^{14}C]-mannitol (plus 100 μM unlabelled); or receiver solutions, identical in composition with the omission of radioisotopes. Samples were taken (50 μl) from receiver compartments after a 1 h incubation and fluxes/permeabilities determined as for T84 cells (see above).

The passive paracellular flux was determined by concurrent measurement of [^{14}C]-mannitol movement. Mannitol is an inert sugar–alcohol and is freely diffusible via the paracellular pathway. Movement of mannitol into the contralateral compartment was generally <2%. Monolayers in which contralateral mannitol movement was >3% were discounted from the results, based on compromised monolayer integrity. Flux calculations were performed as described previously [22,23].

2.4. Real-time quantitative PCR (TaqMan) analysis

Total RNA was isolated as described above and contaminating DNA digested with Turbo DNA-*free*™ (Ambion, Huntingdon, UK). RNA was quantified using a nanodrop ND-1000 spectrophotometer (Nanodrop Technologies Inc., Wilmington, DE, USA) and integrity checked by measurement of the $A_{260/280}$ nm ratio, which was routinely in the range of 1.8–2.0. cDNA synthesis from 1 μg total RNA was performed using the SuperScript™ First-Strand synthesis system (Invitrogen) according to the manufacturers protocol. Product amplification by qPCR was performed with 2 μl cDNA reaction, using qPCR MasterMix plus Low ROX (Eurogentec, Southampton, UK) according to the manufacturer's guidelines. Negative controls involved omission of RNA from the RT reactions and amplification with specific primer/probe sets to confirm the lack of genomic DNA contamination. Human genomic DNA (Roche) was used to produce standard curves for each probe and primer set, allowing absolute quantification. Probes were labeled with 5′-FAM and 3′-DDQ1, purchased from Eurogentec (Southampton, UK). Amplification was performed over 40–50 cycles using the Stratagene MX4000. Data was normalised to the expression of 18s ribosomal RNA. Gene-specific primers and probes were produced for ABCB1 (MDR1), ABCC2 (MRP2), NR1I2 (PXR) and NR1I3 (CAR) and are displayed in Table 1.

2.5. Statistics

Results are expressed as mean ± standard error of mean (S.E.M.) (n). For statistics relating to P_{net}, individual values of net flux from paired monolayers were used. Statistical analysis were performed using Student's unpaired t-tests or one-way analysis of variance (ANOVA) with Bonferroni's post-test for multiple comparisons (GraphPad Instat, San Diego, USA).

Table 1 – Oligonucleotide primer and probe sets used for the amplification of gene expression in T84 cells

Gene	Sequence
ABCB1 (MDR1)	
Forward	5′-GTC CCA GGA GCC CAT CCT-3′
Reverse	5′-CCC GGC TGT TGT CTC CAT A-3′
Probe	5′-TTG ACT GCA GCA TTG CTG AGA ACA TTG C-3′
ABCC2 (MRP2)	
Forward	5′-GGC AGG ACA GGA GCT GGA A-3′
Reverse	5′-GAC CAC CGG CAG CCT CTA A-3′
Probe	5′-TCA TCC CTC ACA AAC TGC CTC TTC AGA ATC-3′
NR1I2 (PXR)	
Forward	5′-CGA GCT CCG CAG CAT CA-3′
Reverse	5′-TGT ATG TCC TGG ATG CGC A-3′
Probe	5′-CGG TGC CAT CCC TTG ACT CAA CCT-3′
NR1I3 (CAR)	
Forward	5′-CCA AAT CCA GCA CAT CCA GG-3′
Reverse	5′-GCC TCA GCT GCA GAT CTC CT-3′
Probe	5′-GTC TGC CAT GAT GCC GCT GCT-3′

3. Results

3.1. Assessment of P-glycoprotein-mediated efflux of xenobiotics across MDR1-MDCK epithelial monolayers

A panel of drug compounds were selected from the literature for their reported ability to interact with MDR1 or PXR (Table 2). The ability of these compounds to act as inhibitors or substrates for hMDR1 was assessed using the hMDR1-transfected MDCKII epithelial monolayers (Tables 3 and 4). Table 3 first demonstrates the increased Pgp-mediated digoxin efflux activity in MDR1-MDCKII cells over the wild-type MDCKII (WT-MDCKII).

Using digoxin as a model Pgp substrate, it can be seen that there is an endogenous net secretory digoxin permeability (P_{net}) in WT-MDCKII cell-layers of 15.2 ± 0.3 cm s^{-1} ($\times 10^{-6}$) and that this is increased to 25.6 ± 1.3 cm s^{-1} ($\times 10^{-6}$) in the MDR1 transfected line ($n = 3$, $P < 0.05$). Mannitol permeabilities (P_{a-b} and P_{b-a}) were not different between WT and MDR1 cell layers (P_{a-b} 1.94 ± 0.11 cm s^{-1} ($\times 10^{-6}$) and 1.87 ± 0.08 cm s^{-1} ($\times 10^{-6}$), $n = 3$, $P > 0.1$, NS; P_{b-a} 2.04 ± 0.11 cm s^{-1} ($\times 10^{-6}$) and 1.98 ± 0.04 cm s^{-1} ($\times 10^{-6}$), $n = 3$, $P > 0.1$, NS for wild-type and MDR1 cells respectively). The increased secretory digoxin flux in the MDR1-MDCKII cells resulted in a marked increase in efflux ratio (P_{b-a}/P_{a-b}) from 7.0 to 11.3 (WT and MDR1-MDCKII respectively, $n = 3$, $P < 0.05$, Table 3). This increase is consistent with the use of digoxin efflux ratio as a measure of Pgp-mediated efflux activity [14].

As a control, the sensitivity of the Pgp-mediated transepithelial digoxin permeability to verapamil inhibition was tested (Table 3); inclusion of 100 μM verapamil resulted in a reduction of net digoxin secretion due to reduced P_{b-a} and increased P_{a-b}, reflected in the reduction in efflux ratios (1.05 ± 0.07 and 1.86 ± 0.07 for WT and MDR1-MDCKII cells respectively ($n = 3$, $P < 0.05$ vs controls, Table 3). Reductions in efflux ratio were observed with mifepristone, clotrimazole, mevastatin and quinidine which corresponded to a reduced P_{net} for digoxin. Smaller reductions in the digoxin efflux ratio were also seen with diltiazem, amprenavir, isradipine, whereas cimetidine and artemisinin, lovostatin, irinotecan, topotecan, atorvastatin and erythromycin displayed no significantly impact on digoxin efflux.

Table 4 summarises the ability of MDR1-MDCKII cell layers to secrete the selected drug compounds by direct determination of asymmetrical permeabilites (see Section 2). Five compounds were found to have efflux ratios (P_{b-a}/P_{a-b}) greater than 3.0, strongly indicating Pgp-mediated active efflux. These were quinidine (32.01), amprenavir (24.20), atorvastatin (8.92), irinotecan (7.11) and erythromycin (4.90). Cimetidine and topotecan displayed efflux ratios of 2.52 and 1.81, respectively, suggesting they may be weak substrates for an efflux transporter. Diltiazem, verapamil and lovastatin have all been classified as Pgp substrates in previous studies [24,25,26], however efflux ratios indicating direct active secretion were not evident. Mifepristone, isradipine, clotrimazole, mevastatin and artemisinin did not display an active secretion in MDR1-MDCKII cell-layers.

Based on the data presented in this study, quinidine is the only compound tested that is both a transported substrate and

Table 2 – Drug compound properties

Drug	MDR1 substrate	MDR1 inhibitor	Gene induction	References
Amprenavir	Y	Y	MDR1	[27,50,51]
Artemisinin	–	–	MDR1, CYP3A4/2B6	[12]
Atorvastatin	Y	Y	–	[52,53]
Cimetidine	Y	–	–	[27,54]
Clotrimazole	–	Y	MDR1, MRP3, CYP3A4	[55,56]
Diltiazem	Y	–	MDR1	[24,27]
Erythromycin	Y	Y	–	[55,57,58]
Irinotecan	Y	–	–	[59]
Isradipine	–	–	CYP3A4	[60]
Lovastatin	Y	Y	–	[26,61]
Mevastatin	–	–	CYP3A4	[13,43]
Mifepristone	–	Y	MRP3, CYP3A4	[4,13,62]
Quinidine	Y	Y	–	[25,27]
Topotecan	Y	–	–	[63]
Verapamil	Y	Y	MDR1	[24,25]

Substrate/inhibitor classifications and induction potential as identified through current literature (see references).

Table 3 – Inhibition of bi-directional digoxin flux across wild-type and MDR1-MDCKII epithelial monolayers

	P_{a-b} ($\times 10^{-6}$ cm s^{-1})	P_{b-a} ($\times 10^{-6}$ cm s^{-1})	P_{net} ($\times 10^{-6} \times$cm s^{-1})	Efflux Ratio (P_{b-a}/P_{a-b})
WT	2.52 ± 0.41	17.71 ± 0.68	15.19 ± 0.28	7.02 ± 0.83
+ Verapamil	3.99 ± 0.39	4.14 ± 0.21	0.15 ± 0.24	1.05 ± 0.07*
MDCK-MDR1	2.49 ± 0.08	28.04 ± 1.28	25.55 ± 1.31	11.26 ± 0.73
+ Verapamil	2.95 ± 0.04	5.47 ± 0.16	2.52 ± 0.20	1.86 ± 0.07*
+ Mifepristone	10.40 ± 1.83	16.42 ± 0.14	6.02 ± 1.74	1.58 ± 0.30*
+ Clotrimazole	7.89 ± 1.88	20.72 ± 1.83	12.83 ± 3.71	2.63 ± 0.80*
+ Mevastatin	3.17 ± 0.45	18.03 ± 0.41	14.88 ± 0.24	5.70 ± 0.06*
+ Quinidine	3.78 ± 1.19	20.59 ± 1.00	16.81 ± 0.77	5.45 ± 0.61*
+ Diltiazem	4.33 ± 0.11	29.90 ± 1.58	25.57 ± 1.61	6.90 ± 0.46*
+ Amprenavir	3.28 ± 0.05	23.39 ± 1.51	20.12 ± 1.48	7.14 ± 0.58*
+ Isradipine	3.47 ± 0.88	25.82 ± 0.49	22.35 ± 1.29	7.44 ± 0.55*
+ Cimetidine	3.06 ± 0.75	24.50 ± 1.03	21.44 ± 1.74	8.00 ± 2.03
+ Artemisinin	3.06 ± 0.18	25.13 ± 1.05	22.08 ± 1.21	8.24 ± 0.80
+ Lovastatin	3.86 ± 0.01	32.55 ± 0.94	28.69 ± 2.10	8.43 ± 0.19
+ Irinotecan	2.89 ± 1.10	26.78 ± 0.56	23.89 ± 0.97	9.27 ± 0.78
+ Topotecan	2.72 ± 0.48	27.28 ± 0.20	24.57 ± 2.02	10.02 ± 1.07
+ Atorvastatin	2.56 ± 0.99	28.94 ± 0.41	26.38 ± 0.92	11.31 ± 0.92
+ Erythromycin	2.71 ± 0.20	33.79 ± 1.18	31.08 ± 1.09	12.45 ± 0.82

Bidirectional transepithelial permeabilities were determined using 0.1 μM [^{3}H]-digoxin and 1 μM [^{14}C]-mannitol with inhibitors added to both apical and basal bathing solutions of MDCKII cell layers. All drug concentrations were 10 μM, with the exception of verapamil (100 μM), cimetidine (50 μM), erythromycin (50 μM) and topotecan (1 μM). Drugs listed in descending inhibitory action on efflux ratio. These concentrations were chosen (with the exception of verapamil) to match the concentrations used for induction of Pgp expression in T84 cells (see Table 5). Data are the mean ± S.E.M. of 3–6 determinations.

* $P < 0.05$ vs controls.

inhibitor of digoxin secretion. Verapamil, clotrimazole, mifepristone and mevastatin may be considered to be non-transported (non)-competitive inhibitors of Pgp. Conversely, amprenavir, atorvastatin, irinotecan and erythromycin appear to be transported substrates but are either weak inhibitors or are not capable of digoxin inhibition. Diltiazem, isradipine, artemisinin and lovastatin are neither transported substrates nor strong inhibitors.

The lack of inhibition by certain compounds previously classified as inhibitors may indicate that the single concentrations used, which were chosen to match those used for the induction studies described in the following section, were not sufficient to block Pgp-mediated efflux. Alternatively, assay type may affect the classification of a compound, as described by Polli et al. [27].

3.2. *Effects of xenobiotic exposure on transepithelial digoxin fluxes in T84 epithelia*

Hyperforin, an active constituent of St. John's Wort, is widely reported to potently activate PXR, resulting in MDR1 and CYP3A4 upregulation [28,29]. Hyperforin was therefore used as

Table 4 – Direct determination of bidirectional transepithelial flux of drug compounds across MDR1-MDCKII epithelial monolayers

Condition	P_{a-b} ($\times 10^{-6}$ cm s^{-1})	P_{b-a} ($\times 10^{-6}$ cm s^{-1})	P_{net} ($P_{b-a} - a-b$)	Efflux ratio (P_{b-a}/P_{a-b})
Quinidine	0.76	24.37	**23.61**	32.01
Amprenavir	1.88	45.44	**43.56**	24.20
Atorvastatin	1.65	14.72	**13.07**	8.92
Irinotecan	0.96	6.85	**5.88**	7.11
Erythromycin	1.30	6.39	**5.09**	4.90
Cimetidine	1.71	4.30	**2.59**	2.52
Topotecan	2.00	3.62	**1.62**	1.81
Diltiazem	10.63	7.57	−3.06	0.71
Verapamil	10.00	6.46	−3.54	0.65
Clotrimazole	4.73	0.85	−3.88	0.18
Isradipine	30.06	25.44	−4.62	0.85
Mifepristone	16.05	11.30	−4.75	0.70
Mevastatin	31.59	23.76	−7.84	0.75
Artemisinin	46.88	37.97	−8.91	0.81
Lovastatin	29.14	13.89	−15.25	0.48

Bidirectional transepithelial and net secretory permeabilities across MDR1-MDCKII cell layers, grown on 96 well transwell supports, were determined for a range of drug compounds. All drugs were tested at a concentration of 10 μM. Compound movement to the contralateral compartment was determined by HPLC MS/MS analysis and expressed as cm s^{-1} ($\times 10^{-6}$). Data are the mean of duplicate wells. Values in bold indicate secreted compounds.

Table 5 – Bidirectional transepithelial digoxin flux across T84 cell monolayers following 72 h xenobiotic exposure

Compound	P_{a-b} ($\times 10^{-6}$ cm s^{-1})	P_{b-a} ($\times 10^{-6}$ cm s^{-1})	P_{net} ($\times 10^{-6}$ cm s^{-1})	Efflux ratio (P_{b-a}/P_{a-b})
Control	1.39 ± 0.06	9.25 ± 0.33	7.86 ± 0.33	6.72 ± 0.26
Mifepristone	1.75 ± 0.06	6.92 ± 0.11	5.19 ± 0.11	4.00 ± 0.15
Cimetidine	0.89 ± 0.06	6.33 ± 0.14	5.44 ± 0.14	7.31 ± 0.53
Verapamil	1.14 ± 0.06	7.72 ± 0.25	6.58 ± 0.22	6.87 ± 0.34
Isradipine	0.81 ± 0.06	8.06 ± 0.33	7.22 ± 0.36	10.2 ± 1.01
Clotrimazole	1.56 ± 0.08	9.03 ± 0.22	7.47 ± 0.25	5.88 ± 0.34
Diltiazem	0.92 ± 0.03	8.44 ± 0.08	7.56 ± 0.08	9.36 ± 0.35
Mevastatin	1.61 ± 0.11	9.58 ± 0.25	8.00 ± 0.33	6.19 ± 0.62
Lovastatin	1.42 ± 0.11	9.56 ± 0.14	8.14 ± 0.14	6.90 ± 0.46
Erythromycin	1.33 ± 0.06	10.17 ± 0.14	**8.83 ± 0.11**	7.70 ± 0.22
Atorvastatin	2.14 ± 0.08	11.22 ± 0.22	**9.08 ± 0.28**	5.34 ± 0.30
Artemisinin	1.61 ± 0.06	10.92 ± 0.19	**9.31 ± 0.22**	6.86 ± 0.25
Quinidine	1.17 ± 0.03	10.44 ± 0.22	**9.28 ± 0.19**	8.99 ± 0.32
Irinotecan	1.36 ± 0.06	12.75 ± 0.44	**11.39 ± 0.47**	9.56 ± 0.69
Topotecan	0.61 ± 0.03	12.42 ± 0.19	**11.81 ± 0.19**	20.3 ± 1.18
Amprenavir	1.08 ± 0.03	13.61 ± 0.75	**12.53 ± 0.75**	12.6 ± 0.85

Bidirectional transepithelial [^{3}H]-digoxin (0.1 μM) permeability was determined across confluent monolayers of T84 cells following 72 h pre-treatment with a range of drug compounds. All drugs were used at a concentration of 10 μM, with the exception of cimetidine (50 μM), erythromycin (50 μM) and topotecan (1 μM). Data are the mean ± S.E.M. of 6 determinations. Values in bold indicate significant induction of P_{net} $P < 0.05$.

a positive control to investigate PXR-mediated MDR1 induction. Pre-treatment of confluent T84 epithelial layers for 72 h with 100 nM hyperforin resulted in a significant induction of digoxin secretion resulting from a 13.6% reduction in apical-to-basal (P_{a-b}, absorptive) digoxin permeability, from 0.59 ± 0.04 cm s^{-1} ($\times 10^{-6}$) control, to 0.51 ± 0.03 cm s^{-1} ($\times 10^{-6}$) hyperforin treated, ($n = 6$, $P < 0.05$), and a 26.8% increase in basal-to-apical (P_{b-a}, secretory) digoxin permeability (6.22 ± 0.19 cm s^{-1} ($\times 10^{-6}$) control, to 7.89 ± 0.19 cm s^{-1} ($\times 10^{-6}$) hyperforin treated, ($n = 6$, $P < 0.05$). This increased the digoxin efflux ratio (45.5%) in T84 cells from 11.0 ± 1.2 to 16.0 ± 1.1 ($n = 6$, $P < 0.05$).

The ability of each of the drug compounds to induce functional P-glycoprotein expression was similarly assessed (see Table 5 for details). Significant increases in net secretory digoxin permeability over control levels (7.86 ± 0.33 cm s^{-1} ($\times 10^{-6}$), $n = 6$) were recorded following pre-treatment with erythromycin (12.3%), irinotecan (44.9%) and artemisinin (18.4%). The increases in net permeability were the result of significant increases in control basal-to-apical (P_{b-a}) permeability (9.25 ± 0.33 cm s^{-1} ($\times 10^{-6}$)) by 9.9% (erythromycin), 37.8% (irinotecan) and 18.1% (artemisinin, $n = 6$, $P < 0.05$).

Increased net secretory digoxin movement in T84 cells was also found following pre-treatment with quinidine (18.1%), amprenavir (59.4%) and topotecan (50.3%, $n = 6$). The increased net flux following pre-treatment with these drug compounds was the result of a reduction in absorptive (P_{a-b}) permeability in relation to controls (1.39 ± 0.06 cm s^{-1} ($\times 10^{-6}$)) by 15.9% (quinidine), 22.3% (amprenavir) and 56.1% (topotecan, $n = 6$, $P < 0.05$) as well as increases in secretory (P_{b-a}) permeability by 12.9% (quinidine), 47.1% (amprenavir) and 34.3% (topotecan) when compared to the control value (9.25 ± 0.33 cm s^{-1} ($\times 10^{-6}$), $n = 6$, $P < 0.05$). The increased digoxin efflux ratios that are demonstrated following pre-treatment with isradipine (51.8%), diltiazem (33.9%), irinotecan (42.3%), quinidine (33.8%), amprenavir (87.5%) and topotecan (202.1%) are equivalent to the increases seen in the hMDR1 over-expressing MDCKII cell layers (60.4%) (Table 3) suggesting increased MDR1 expression ($n = 6$, $P < 0.05$).

Pre-treatment of T84 cell monolayers with mifepristone (10 μM), cimetidine (50 μM) and verapamil (10 μM) resulted in significant reductions in net digoxin permeability by 34.0% (mifepristone), 30.5% (cimetidine) and 16.3% (verapamil, $n = 6$, $P < 0.05$). The reduction in net digoxin permeability (P_{net}) was primarily the result of a fall in secretory (basal-to-apical, P_{b-a}) permeability following mifepristone (25.2%), cimetidine (31.6%) and verapamil (16.5%) exposure ($n = 6$, $P < 0.05$). Mifepristone pre-treatment also resulted in a significant increase in absorptive (apical-to-basal, P_{a-b}) digoxin permeability (25.9%), with cimetidine and verapamil reducing P_{a-b} 36.0% and 18.0%, respectively ($n = 6$, $P < 0.06$).

Atorvastatin (10 μM), isradipine (10 μM), diltiazem (10 μM), mevastatin (10 μM), lovastatin (10 μM) and clotrimazole (10 μM) exposure did not affect net digoxin permeability in T84 layers. The uni-directional fluxes indicate that absorptive digoxin permeability was reduced following isradipine (41.7%) and diltiazem (33.8%) pre-treatment, as was secretory digoxin permeability (12.9% and 0.8%, respectively, $n = 6$, $P < 0.05$). The overall reduction in digoxin flux is likely the result of a decreased paracellular component as opposed to drug treatment. T84 layers displayed higher transepithelial electrical resistances (TEER) following isradipine (688 ± 21 Ω cm^2) and diltiazem (836 ± 36 Ω cm^2) exposure in comparison to control layers (524 ± 15 Ω cm^2, $n = 12$, $P < 0.05$). This is correlated with reduced mannitol permeability following xenobiotic exposure (7.72 ± 0.50 cm s^{-1} ($\times 10^{-6}$) control, 4.78 ± 0.47 cm s^{-1} ($\times 10^{-6}$) isradipine, 4.91 ± 0.42 cm s^{-1} ($\times 10^{-6}$) diltiazem, $n = 12$, $P < 0.05$).

The Venn diagram shown in Fig. 3 summarises the ability of each of the selected drug compounds to act as a secreted substrate, an inhibitor or inducer of P-glycoprotein.

3.3. *Impact of xenobiotic treatment on MDR1, MRP2, PXR and CAR gene expression in T84 cells*

Real-time quantitative PCR confirms co-expression of MDR1 with PXR mRNA ($1.70 \pm 0.37 \times 10^6$ copies/μg RNA and $3.28 \pm 0.41 \times 10^6$ copies/μg RNA for MDR1 and PXR respectively, $n = 9$). The impact of xenobiotic exposure on MDR1 and MRP2 mRNA expression levels was determined following 72 h pre-treatment of T84 epithelial layers. Hyperforin increased MDR1 transcript levels 3.0 fold ($n = 4$, $P < 0.05$) but had no impact on MRP2 mRNA expression ($n = 4$, $P > 0.1$ NS), suggesting that PXR-mediated induction of MDR1 transcript levels upregulates functional MDR1 protein levels and transepithelial fluxes (see above).

Quinidine and topotecan had a similar action to hyperforin in displaying significant stimulation of functional activity and induction of MDR1 mRNA expression with 3.80 ± 0.97 and 2.29 ± 0.18 fold increases over control values respectively ($n = 4$, $P < 0.05$) (Fig. 1). Of the compounds investigated, amprenavir induces the largest increase in Pgp functional activity (see Table 5) and, as is shown in Fig. 1, also increases MDR1 gene expression (5.05 ± 2.13 fold, $n = 3$, $P > 0.1$, NS), although this is not statistically significant. Erythromycin, irinotecan and artemisinin all show significant increases in MDR1 functional activity (displaying 1.12 ± 0.05, 1.45 ± 0.06, 1.18 ± 0.04, fold increases in net digoxin flux respectively, $n = 4$, $P < 0.05$) but had no effect on MDR1 transcript levels (erythromycin 0.42 ± 0.11, irinotecan 1.09 ± 0.21 and artemisinin 1.24 ± 0.39 fold change in relation to controls) indicating post-transcriptional regulation of digoxin secretion. Mifepristone, cimetidine and verapamil, all compounds that significantly reduced net digoxin flux after 72 h pre-incubation, had no impact on MDR1 transcript levels. This indicates the functional impact is not the result of a reduction in gene transcription. Of the drug compounds that had no impact on overall digoxin flux, mevastatin alone had a significant effect on MDR1 gene expression, displaying a 2.45 ± 0.56 fold increase in mRNA levels over control treatment ($n = 4$, $P < 0.05$).

The effect of drug exposure on MRP2 expression levels was somewhat different to MDR1. Both of the topoisomerase inhibitors under investigation significantly reduced MRP2

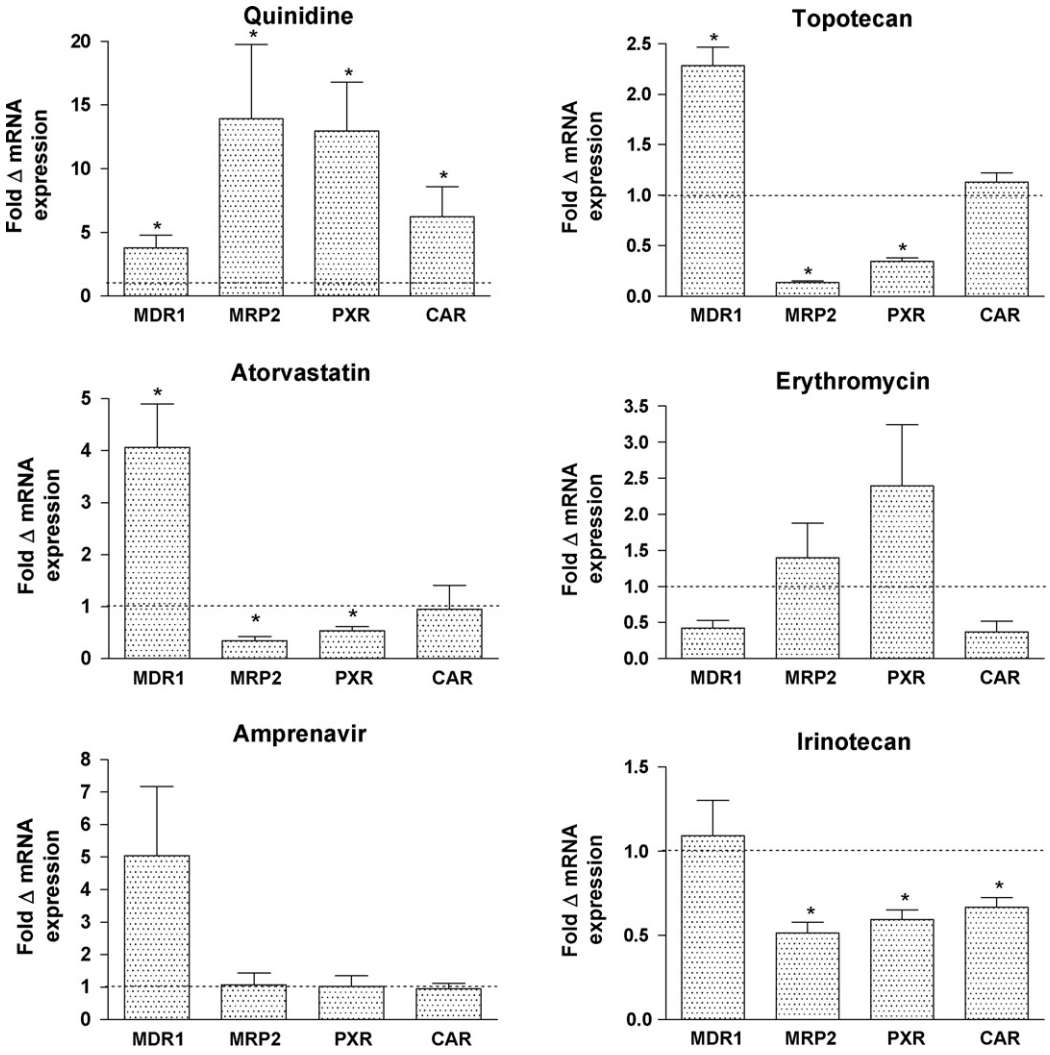

Fig. 1 – Changes in MDR1, MRP2, PXR and CAR mRNA levels relative to controls were determined by real-time PCR (TaqMan) following 72 h xenobiotic pre-treatment in T84 cells. All drug concentrations were 10 μM, with the exception of topotecan (1 μM) and erythromycin (50 μM) (significance indicated by * $P < 0.05$, $n = 4$).

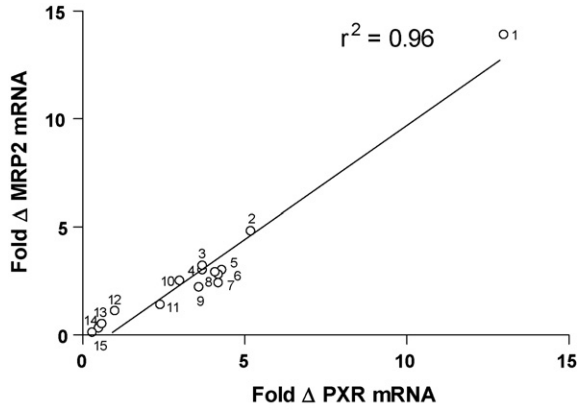

Fig. 2 – Relationship between fold change in MRP2 and PXR expression following 72 h xenobiotic pre-treatment. Linear regression analysis indicates a significant positive correlation between xenobiotic exposure and modulation of MRP2 and PXR gene expression. (1) Quinidine, (2) Isradipine, (3) Diltiazem, (4) Cimetidine, (5) Mevastatin, (6) Lovastatin, (7) Verapamil, (8) Artemisinin, (9) Clotrimazole, (10) Mifepristone, (11) Erythromycin, (12) Amprenavir, (13) Irinotecan, (14) Atorvastatin, (15) Topotecan. Data are mean of $n = 4$ separate cell layers, $r^2 = 0.96$, $P < 0.05$.

mRNA expression, with irinotecan lowering levels to 0.52 ± 0.06 and topotecan to 0.14 ± 0.02 of control values. Atorvastatin also reduced MRP2 expression to 0.42 ± 0.13 fold of controls. Otherwise MRP2 mRNA levels were increased; significant increases being observed with cimetidine (2.98 ± 0.76 fold) and quinidine (13.9 ± 5.84 fold). Increased MRP2 expression would not have impacted on digoxin flux however, as the cardiac glycoside is not a substrate for MRP2 [14]. Changes in the mRNA expression levels of the nuclear xenobiotic receptors PXR and CAR was also assessed following 72 h drug exposure. Increases in PXR expression were seen for the majority of the compounds investigated. Significant fold increases in PXR transcript levels above control were seen following exposure to mifepristone (3.03 ± 0.87), cimetidine (3.70 ± 1.19), verapamil (4.15 ± 1.21), isradipine (5.22 ± 2.06), mevastatin (4.31 ± 1.18), lovastatin (4.23 ± 1.47), clotrimazole (3.61 ± 1.01), artemisinin (4.05 ± 1.21) and quinidine (13.0 ± 3.80) ($n = 4$, $P < 0.05$). Atorvastatin, irinotecan and topotecan exposure resulted in a reduction of PXR mRNA levels to 0.53 ± 0.08, 0.60 ± 0.06 and 0.35 ± 0.03 of control values, respectively ($n = 4$, $P < 0.05$). Diltiazem, erythromycin and amprenavir were without effect on PXR transcript levels.

The result of xenobiotic exposure on CAR expression was markedly different. Quinidine was alone in significantly increasing mRNA expression, displaying a 6.26 ± 2.36 fold increase above control values ($n = 4$, $P < 0.05$). Irinotecan exposure resulted in reduced CAR expression, with transcript levels falling to 0.67 ± 0.06 of control values ($n = 4$, $P < 0.05$).

Changes in PXR and MRP2 expression following xenobiotic exposure followed a remarkably similar pattern. Fig. 2 displays the relationship between fold increases in the transcript levels of each gene, with linear regression analysis indicating a strong correlation ($r^2 = 0.96$, $n = 4$, $P < 0.05$).

4. Discussion

The present study was undertaken to determine the effects of a range of xenobiotics on the function and expression of Pgp, along with the expression of the 'xenosensing' nuclear receptors responsible for MDR1 transcriptional regulation. The involvement of Pgp in the active efflux of an extremely diverse range of compounds is now well established [1,27]. It is acknowledged that efflux transporters may play a role in a number of drug–drug interactions and avoiding this phenomenon is becoming increasingly important in the development of new chemical entities (NCEs) by the pharmaceutical industry. Assessing Pgp function and regulation has often involved the use of cultured cell models [30], gene expression studies [31] and reporter gene assays [19]. However, in order for gene expression data to be validated it must be coupled with the functional assessment of Pgp-mediated activity. The most direct measure of transport processes in vitro involves the use of confluent, polarised epithelial cell-lines, reconstituted onto permeable supports to allow the assessment of transcellular (absorptive and secretory) and paracellular components [27,20,32]. We have previously described the use of the T84 intestinal adenocarcinoma cultured cell line, as a model for assessing PXR-mediated induction of Pgp [18]. As well as expressing both MDR1 and PXR genes, T84 cells display asymmetrical, verapamil-sensitive, digoxin transport that is increased by pre-incubation with the PXR-activator rifampin. An active constituent of the herbal remedy St. John's Wort (SJW), hyperforin, has also been reported to be a potent PXR activator, resulting in the upregulation of MDR1 [28]. This has significant clinical relevance, as shown by reports of the harmful interaction between SJW and certain medications, the most widely reported of which is the immunosuppressant and Pgp substrate cyclosporine A (CsA), generally administered following organ transplantation [7]. Increases in Pgp expression following SJW ingestion have been reported, reducing the plasma AUC of CsA and increasing the risk of allograft rejection [7,33,34]. Here we demonstrate that pre-incubation of T84 cells for 72 h with hyperforin (100 nM) results in a significant increase in secretory digoxin movement, coupled to an increase in MDR1 transcript levels. This is consistent with previous reports of hyperforin activity [28] and further highlights the ability of the T84 model to mimic the in vivo situation.

Using the MDR1-overexpressing MDCKII cell line, we have directly determined which of a panel of drug compounds are subject to transepithelial secretion, most likely as a result of being Pgp substrates; these compounds are cimetidine, atorvastatin, erythromycin, irinotecan, quinidine, amprenavir and topotecan. The drug compounds were also screened for their ability to inhibit Pgp-mediated digoxin efflux in MDR1-MDCKII cells. Significant inhibition of Pgp activity was observed with verapamil, mifepristone (RU486), clotrimazole, mevastatin and quinidine. All of these compounds, with the exception of mevastatin, have previously been described as Pgp inhibitors (see Table 2). The structural basis for substrate and modulator recognition by Pgp is complex, as demonstrated by the breadth of literature dedicated to this topic. P-glycoprotein has been reported to display at least 2 functional drug binding sites, known as the H-site and R-site (preferen-

tially binding Hoescht 33342 and rhodamine 123, respectively) [35]. However, at least four separate binding sites are speculated [36], described as either transport or modulatory sites. Inhibition of Pgp activity can result from competition for active transport sites or allosteric regulation involving binding to distinct modulatory sites [36]. Verapamil is thought to attenuate Pgp-mediated transport through competitive inhibition of transport sites within the ligand binding domain [37,38]. Conversely, XR9576, a third generation non-transported Pgp inhibitor, is reported to interact with a distinct modulatory binding site, inhibiting ATPase activity [36,39]. The distinction between verapamil and XR9576 action is highlighted by the fact that verapamil potently stimulates ATPase activity, further evidence that the calcium channel blocker associates with a site distinct from the modulatory site bound by XR9576 [39,40]. Allosteric modulation is speculated to alter the equilibrium between high and low affinity states of the binding sites, resulting from the conformational change that results following the interaction of a compound with a specific site [15]. The complexity of the interactions between binding sites was demonstrated by Pascaud et al. [40], indicating an array of cross-modulation between at least 4 distinct binding sites, postulated to explain the broad substrate interactions exhibited by Pgp. A comprehensive report by Polli et al. [27] described the classification of substrates or modulators as being dependent on the type of assay used in the study (bidirectional flux, ATPase or calcein-AM efflux). Of the compounds found to undergo net Pgp-mediated efflux in the present study, erythromycin, cimetidine, irinotecan and atorvastatin do not show marked inhibition of digoxin efflux (see Fig. 3). It could therefore be speculated that these compounds interact with a binding site distinct from that of digoxin. Alternatively, low binding affinities could prevent significant displacement of digoxin, as has previously been suggested for erythromycin, cimetidine and a range of other drug compounds found to show asymmetrical Pgp-mediated transport but not inhibition of Calcein-AM efflux [27]. The recognition and binding of substrates and modulators by Pgp remains an area of debate. The exact number of binding sites and the mechanisms for substrate/modulator binding affecting conformation, affinity and transport activity is yet to be unambiguously defined.

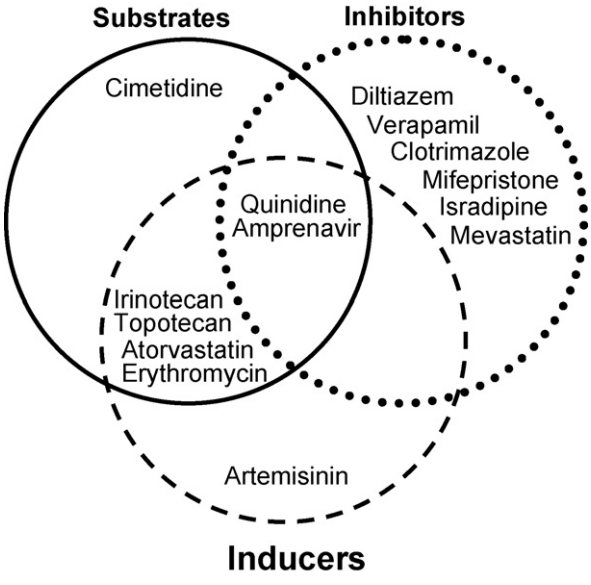

Fig. 3 – Venn diagram indicating the interaction of each of the panel of drug compounds with Pgp as a substrate or inhibitor as well as their ability to induce Pgp activity. The solid circle indicates compounds shown to be Pgp substrates, the dotted circle compounds shown to be Pgp inhibitors and the dashed circle compounds that induce Pgp expression.

It is evident from this study that although Pgp and PXR display a significant degree of overlap in substrate specificities, the relationship between substrate activity and induction is not straightforward. Fig. 3 shows a Venn diagram defining the drugs investigated as either ''Inducer'', ''Inhibitor'' or ''Substrate'' of Pgp. Based on the present study, only quinidine and amprenavir were classified as competitive substrates (displaying both substrate activity and inhibition) inducing Pgp activity. Most compounds defined as substrates acted to induce Pgp activity (atorvastatin, erthyromycin, irinotecan and topotecan), but did not always show inhibition. Artemsinin was the exception, displaying no net active secretion in the MDR1-MDCKII model, but inducing Pgp activity on pre-exposure of the T84 cell-line. Of those drug compounds defined as inhibitors, most (verapamil, mifepristone, clotrimazole, mevastatin, diltiazem and isradipine) did not act as inducers to increase Pgp activity (Fig. 3).

It may be assumed that the ability of a drug compound to induce Pgp activity will be related to an increase in MDR1 mRNA expression, if mediated by increased PXR-dependent transcription, as is the case with hyperforin. Quinidine, topotecan, atorvastatin and amprenavir all increased MDR1 expression. However the increments in functional activity observed with erythromycin, irinotecan and artemisinin, are not associated with increased MDR1 mRNA levels. Conversely mevastatin which does not induce functional activity increases MDR1 mRNA levels. It is therefore apparent that although increments in MDR1 mRNA levels may result in increased functional activity, post-transcriptional regulation also plays an important role in determining functional effects. Recently, it has been reported that MDR1 mRNA translation is blocked in K562 leukaemia cells following cytotoxic drug treatment. Despite this increase in MDR1 mRNA levels, it was reported that a structured fold in the 5′-end of MDR1 reduces its ability to compete with the translation machinery when the akt pathway is stimulated by cytotoxic stress [41]. Additional mechanisms may also operate at the level of protein traffic to the plasma membrane and at the level of transport activity (i.e. phosphorylation) [42].

A number of nuclear receptors are recognised to be involved in MDR1 transcriptional regulation and as such, increases in expression and activity cannot be definitively related to PXR alone [11,12]. Moore et al. [15] gave an insight into the degree of overlap in ligand specificity between PXR and CAR suggesting the net effect of a particular xenobiotic was likely to be dependent on both PXR and CAR transcriptional cascades. As PXR and CAR are now known to interact with the same DR3, DR4, ER6 and ER8 response elements [9,43,44,45], significant overlap in transcriptional activity is possible.

Somewhat surprisingly, there was significant modulation of PXR expression itself, with 12 of the 15 drugs investigated altering PXR transcript levels. It is already clear that the ligand binding domain of PXR allows for a broad structural promiscuity [46] and the diverse range of drug entities that alter PXR expression levels in the T84 cell line would agree with this evaluation. The promiscuity of PXR has been described as directed rather than random, as suggested by species-specific ligand activation. The most notable examples of species specificity are rifampin, an efficient PXR activator in humans but a very weak activator of murine PXR, and pregnenolone 16α-carbonitrile (PCN) which activates the rodent, but not human PXR [47,48]. This activational disparity results from distinct ligand binding domains, with mPXR displaying only 74–78% sequence homology with the hPXR ligand binding domain [47,48]. Maglich and colleagues [11] reported the ability of murine PXR to auto-regulate expression in response to PCN dosing. It cannot be clearly determined whether auto- or cross-regulation is responsible for changes in PXR expression in this study. What is clear is that the impact on CAR transcription is notably different. Irinotecan and quinidine are the exceptions, displaying down-regulation and upregulation of both receptors, respectively. Although previous research has shown that CAR activation has the ability to reduce PXR expression [17], further investigation would be required to confirm the involvement of CAR in PXR regulation in the T84 system.

Another efflux transporter regulated by PXR is MRP2 [10]. We have shown here that changes in MRP2 expression are distinct from that of MDR1 expression. It has been reported that PXR, FXR and CAR are all capable of regulating MRP2 gene expression in response to ligand binding [10]. As such it is unclear whether exposure to drug compounds and the resultant modulation of MRP2 expression is mediated by one or all of these nuclear receptors. Of the drugs that increase MDR1 expression, only quinidine has a similar impact on MRP2 transcription. The effects of topotecan and atorvastatin exposure are in fact opposite, with increased MDR1 and reduced MRP2 expression. Interestingly, both compounds also down-regulate PXR whilst having no impact on CAR expression. As the action of each nuclear receptor is governed by the recruitment of co-activators or co-repressors [49], it is possible that the up- and downregulation may result from such interactions. Given the increasing number of reports indicating cross-talk between nuclear receptors [17], it is also possible that a network of receptors acts in concert to alter gene expression. This would effectively amplify the potential for the body to respond to xenobiotic insult and allow for the response to an even broader range of structurally diverse compounds.

The relationship between modulation of MRP2 and PXR mRNA expression levels is striking. The strong correlation between fold-changes in expression following xenobiotic exposure suggests very similar or identical mechanisms of regulation. Whether this involves ligand-induced recruitment of a complimentary set of nuclear receptors or cofactors is however, unclear.

This study has identified the human intestinal T84 cell-line as an appropriate model for investigating induction of Pgp activity. The results also highlight the complexity of the cellular response to individual drug exposure. Whilst the complement of nuclear receptors, efflux transporters and metabolising enzymes present in the enterocytes provides an efficient and adaptable barrier against exogenous compounds, the present data indicate that the impact of exposure to drug compounds will need to be assessed on a case-by-case basis.

Acknowledgements

We are grateful to Clare Summers at AstraZeneca for her support with the TaqMan analysis. TaqMan probe and primer sequences were kindly supplied by Katherine Howe (University of Surrey). This work was supported by a BBSRC CASE studentship award in conjunction with AstraZeneca.

REFERENCES

[1] Marchetti S, Mazzanti R, Beijnen JH, Schellens JH. Concise review: clinical relevance of drug–drug and herb–drug interactions mediated by the ABC transporter ABCB1 (MDR1 P-glycoprotein). Oncologist 2007;12:927–41.
[2] Igel S, Drescher S, Murdter T, Hofmann U, Heinkele G, Tegude H, et al. Increased absorption of digoxin from the human jejunum due to inhibition of intestinal transporter-mediated efflux. Clin Pharmacokinet 2007;46:777–85.
[3] Meerum Terwogt JM, Beijnen JH, ten Bollel Huinink WW, Rosing H, Schellens JHM. Co-administration of cyclosporin enables oral therapy with paclitaxel. Lancet 1998;352:285.
[4] Woodland C, Koren G, Ito S. From bench to bedside: utilization of an in vitro model to predict potential drug–drug interactions in the kidney: the digoxin-mifepristone example. J Clin Pharmacol 2003;43:743–50.
[5] Westphal K, Weinbrenner A, Zschiesche M, Franke G, Knoke M, Oertel R, et al. Induction of P-glycoprotein by rifampin increases intestinal secretion of talinolol in human beings: a new type of drug/drug interaction. Clin Pharmacol Ther 2000;68:345–55.
[6] Drescher S, Glaeser H, Murdter T, Hitzl M, Eichelbaum M, Fromm MF. P-glycoprotein-mediated intestinal and biliary digoxin transport in humans. Clin Pharmacol Ther 2003;73:223–31.
[7] Ruschitzka F, Meier PJ, Turina M, Luscher TF, Noll G. Acute heart transplant rejection due to Saint John's wort. Lancet 2000;355:548–9.
[8] Ernst E. Herb–drug interactions: potentially important but woefully under-researched. Eur J Clin Pharmacol 2000;56:523–4.
[9] Handschin C, Meyer UA. Induction of drug metabolism: the role of nuclear receptors. Pharmacol Rev 2003;55:649–73.
[10] Kast HR, Goodwin B, Tarr PT, Jones SA, Anisfeld AM, Stoltz CM, et al. Regulation of multidrug resistance-associated protein 2 (ABCC2) by the nuclear receptors pregnane X receptor, farnesoid X-activated receptor, and constitutive androstane receptor. J Biol Chem 2002;277:2908–15.
[11] Maglich JM, Stoltz CM, Goodwin B, Hawkins-Brown D, Moore JT, Kliewer SA. Nuclear pregnane x receptor and constitutive androstane receptor regulate overlapping but distinct sets of genes involved in xenobiotic detoxification. Mol Pharmacol 2002;62:638–46.
[12] Burk O, Arnold KA, Geick A, Tegude H, Eichelbaum M. A role for constitutive androstane receptor in the regulation of human intestinal MDR1 expression. Biol Chem 2005;386:503–13.

[13] Raucy J, Warfe L, Yueh MF, Allen SW. A cell-based reporter gene assay for determining induction of CYP3A4 in a high-volume system. J Pharmacol Exp Ther 2002;303:412–23.
[14] Taipalensuu J, Tavelin S, Lazorova L, Svensson AC, Artursson P. Exploring the quantitative relationship between the level of MDR1 transcript, protein and function using digoxin as a marker of MDR1-dependent drug efflux activity. Eur J Pharm Sci 2004;21:69–75.
[15] Moore LB, Parks DJ, Jones SA, Bledsoe RK, Consler TG, Stimmel JB, et al. Orphan nuclear receptors constitutive androstane receptor and pregnane X receptor share xenobiotic and steroid ligands. J Biol Chem 2000;275: 15122–7.
[16] Orans J, Teotico DG, Redinbo MR. The nuclear xenobiotic receptor pregnane X receptor: recent insights and new challenges. Mol Endocrinol (Baltimore MD) 2005;19: 2891–900.
[17] Gibson GG, Phillips A, Aouabdi S, Plant K, Plant N. Transcriptional regulation of the human pregnane-X receptor. Drug Metab Rev 2006;38:31–49.
[18] Haslam IS, Jones K, Coleman T, Simmons NL. Rifampin and digoxin induction of MDR1 expression and function in human intestinal (T84) epithelial cells. Br J Pharmacol 2008;154:246–55.
[19] Madara JL, Stafford J, Dharmsathaphorn K, Carlson S. Structural analysis of a human intestinal epithelial cell line. Gastroenterology 1987;92:1133–45.
[20] Hunter J, Hirst BH, Simmons NL. Epithelial secretion of vinblastine by human intestinal adenocarcinoma cell (HCT-8 and T84) layers expressing P-glycoprotein. Br J Cancer 1991;64:437–44.
[21] Horio M, Chin KV, Currier SJ, Goldenberg S, Williams C, Pastan I, et al. Transepithelial transport of drugs by the multidrug transporter in cultured Madin-Darby canine kidney cell epithelia. J Biol Chem 1989;264:14880–4.
[22] Cavet ME, West M, Simmons NL. Transport and epithelial secretion of the cardiac glycoside, digoxin, by human intestinal epithelial (Caco-2) cells. Br J Pharmacol 1996;118:1389–96.
[23] Cavet ME, West M, Simmons NL. Fluoroquinolone (ciprofloxacin) secretion by human intestinal epithelial (Caco-2) cells. Br J Pharmacol 1997;121:1567–78.
[24] Herzog CE, Tsokos M, Bates SE, Fojo AT. Increased mdr-1/P-glycoprotein expression after treatment of human colon carcinoma cells with P-glycoprotein antagonists. J Biol Chem 1993;268:2946–52.
[25] Collett A, Tanianis-Hughes J, Warhurst G. Rapid induction of P-glycoprotein expression by high permeability compounds in colonic cells in vitro: a possible source of transporter mediated drug interactions? Biochem Pharmacol 2004;68:783–90.
[26] Chen Y, Kissling G, Negishi M, Goldstein JA. The nuclear receptors constitutive androstane receptor and pregnane X receptor cross-talk with hepatic nuclear factor 4alpha to synergistically activate the human CYP2C9 promoter. J Pharmacol Exp Ther 2005;314:1125–33.
[27] Polli JW, Wring SA, Humphreys JE, Huang L, Morgan JB, Webster LO, et al. Rational use of in vitro P-glycoprotein assays in drug discovery. J Pharmacol Exp Ther 2001;299:620–8.
[28] Durr D, Stieger B, Kullak-Ublick GA, Rentsch KM, Steinert HC, Meier PJ, et al. St John's Wort induces intestinal P-glycoprotein/MDR1 and intestinal and hepatic CYP3A4. Clin Pharmacol Ther 2000;68:598–604.
[29] Tannergren C, Engman H, Knutson L, Hedeland M, Bondesson U, Lennernas H. St John's wort decreases the bioavailability of R- and S-verapamil through induction of the first-pass metabolism. Clin Pharmacol Ther 2004;75:298–309.
[30] Lowes S, Cavet ME, Simmons NL. Evidence for a non-MDR1 component in digoxin secretion by human intestinal Caco-2 epithelial layers. Eur J Pharmacol 2003;458:49–56.
[31] Englund G, Rorsman F, Ronnblom A, Karlbom U, Lazorova L, Grasjo J, et al. Regional levels of drug transporters along the human intestinal tract: co-expression of ABC and SLC transporters and comparison with Caco-2 cells. Eur J Pharm Sci 2006;29:269–77.
[32] Lowes S, Simmons NL. Multiple pathways for fluoroquinolone secretion by human intestinal epithelial (Caco-2) cells. Br J Pharmacol 2002;135:1263–75.
[33] Moschella C, Jaber BL. Interaction between cyclosporine and Hypericum perforatum (St. John's wort) after organ transplantation. Am J Kidney Dis 2001;38:1105–7.
[34] Bauer S, Stormer E, Johne A, Kruger H, Budde K, Neumayer HH, et al. Alterations in cyclosporin A pharmacokinetics and metabolism during treatment with St John's wort in renal transplant patients. Br J Clin Pharmacol 2003;55:203–11.
[35] Sharom FJ, Lugo MR, Eckford PD. New insights into the drug binding, transport and lipid flippase activities of the p-glycoprotein multidrug transporter. J Bioenerg Biomembr 2005;37:481–7.
[36] Martin C, Berridge G, Higgins CF, Mistry P, Charlton P, Callaghan R. Communication between multiple drug binding sites on P-glycoprotein. Mol Pharmacol 2000;58:624–32.
[37] Garrigos M, Mir LM, Orlowski S. Competitive and non-competitive inhibition of the multidrug-resistance-associated P-glycoprotein ATPase—further experimental evidence for a multisite model. Eur J Biochem 1997;244: 664–73.
[38] Litman T, Zeuthen T, Skovsgaard T, Stein WD. Competitive, non-competitive and cooperative interactions between substrates of P-glycoprotein as measured by its ATPase activity. Biochim Biophys Acta 1997;1361:169–76.
[39] Martin C, Berridge G, Mistry P, Higgins C, Charlton P, Callaghan R. The molecular interaction of the high affinity reversal agent XR9576 with P-glycoprotein. Br J Pharmacol 1999;128:403–11.
[40] Pascaud C, Garrigos M, Orlowski S. Multidrug resistance transporter P-glycoprotein has distinct but interacting binding sites for cytotoxic drugs and reversing agents. Biochem J 1998;333(Pt 2):351–8.
[41] Randle RA, Raguz S, Higgins CF, Yague E. Role of the highly structured 5′-end region of MDR1 mRNA in P-glycoprotein expression. Biochem J 2007;406:445–55.
[42] Kim H, Barroso M, Samanta R, Greenberger L, Sztul E. Experimentally induced changes in the endocytic traffic of P-glycoprotein alter drug resistance of cancer cells. Am J Physiol 1997;273:C687–702.
[43] Sueyoshi T, Kawamoto T, Zelko I, Honkakoski P, Negishi M. The repressed nuclear receptor CAR responds to phenobarbital in activating the human CYP2B6 gene. J Biol Chem 1999;274:6043–6.
[44] Xie W, Barwick JL, Simon CM, Pierce AM, Safe S, Blumberg B, et al. Reciprocal activation of xenobiotic response genes by nuclear receptors SXR/PXR and CAR. Genes Dev 2000;14:3014–23.
[45] Goodwin B, Moore LB, Stoltz CM, McKee DD, Kliewer SA. Regulation of the human CYP2B6 gene by the nuclear pregnane X receptor. Mol Pharmacol 2001;60:427–31.
[46] Watkins RE, Wisely GB, Moore LB, Collins JL, Lambert MH, Williams SP, et al. The human nuclear xenobiotic receptor PXR: structural determinants of directed promiscuity. Science 2001;292:2329–33.
[47] Bertilsson G, Heidrich J, Svensson K, Asman M, Jendeberg L, Sydow-Backman M, et al. Identification of a human nuclear receptor defines a new signaling pathway for CYP3A induction. Proc Natl Acad Sci USA 1998;95:12208–13.

[48] Lehmann JM, McKee DD, Watson MA, Willson TM, Moore JT, Kliewer SA. The human orphan nuclear receptor PXR is activated by compounds that regulate CYP3A4 gene expression and cause drug interactions. J Clin Invest 1998;102:1016–23.
[49] Eloranta JJ, Kullak-Ublick GA. Coordinate transcriptional regulation of bile acid homeostasis and drug metabolism. Arch Biochem Biophys 2005;433:397–412.
[50] Perloff MD, von Moltke LL, Fahey JM, Daily JP, Greenblatt DJ. Induction of P-glycoprotein expression by HIV protease inhibitors in cell culture. AIDS (London England) 2000;14:1287–9.
[51] Storch CH, Theile D, Lindenmaier H, Haefeli WE, Weiss J. Comparison of the inhibitory activity of anti-HIV drugs on P-glycoprotein. Biochem Pharmacol 2007;73:1573–81.
[52] Hochman JH, Pudvah N, Qiu J, Yamazaki M, Tang C, Lin JH, et al. Interactions of human P-glycoprotein with simvastatin, simvastatin acid, and atorvastatin. Pharm Res 2004;21:1686–91.
[53] Rodrigues AC, Curi R, Britto LR, Rebbechi IM, Hirata MH, Bertolami MC, et al. Down-regulation of ABCB1 transporter by atorvastatin in a human hepatoma cell line and in human peripheral blood mononuclear cells. Biochim Biophys Acta 2006;1760:1866–73.
[54] Romiti N, Tramonti G, Chieli E. Influence of different chemicals on MDR-1 P-glycoprotein expression and activity in the HK-2 proximal tubular cell line. Toxicol Appl Pharmacol 2002;183:83–91.
[55] Schuetz EG, Beck WT, Schuetz JD. Modulators and substrates of P-glycoprotein and cytochrome P4503A coordinately up-regulate these proteins in human colon carcinoma cells. Mol Pharmacol 1996;49:311–8.
[56] Teng S, Jekerle V, Piquette-Miller M. Induction of ABCC3 (MRP3) by pregnane X receptor activators. Drug Metab Dispos 2003;31:1296–9.
[57] Chan LM, Cooper AE, Dudley AL, Ford D, Hirst BH. P-glycoprotein potentiates CYP3A4-mediated drug disappearance during Caco-2 intestinal secretory detoxification. J Drug Target 2004;12:405–13.
[58] Eriksson UG, Dorani H, Karlsson J, Fritsch H, Hoffmann KJ, Olsson L, et al. Influence of erythromycin on the pharmacokinetics of ximelagatran may involve inhibition of P-glycoprotein-mediated excretion. Drug Metab Dispos 2006;34:775–82.
[59] Iyer L, Ramirez J, Shepard DR, Bingham CM, Hossfeld DK, Ratain MJ, et al. Biliary transport of irinotecan and metabolites in normal and P-glycoprotein-deficient mice. Cancer Chemother Pharmacol 2002;49:336–41.
[60] Drocourt L, Pascussi JM, Assenat E, Fabre JM, Maurel P, Vilarem MJ. Calcium channel modulators of the dihydropyridine family are human pregnane X receptor activators and inducers of CYP3A, CYP2B, and CYP2C in human hepatocytes. Drug Metab Dispos 2001;29:1325–31.
[61] Sakaeda T, Takara K, Kakumoto M, Ohmoto N, Nakamura T, Iwaki K, et al. Simvastatin and lovastatin, but not pravastatin, interact with MDR1. J Pharm Pharmacol 2002;54:419–23.
[62] Trubetskoy O, Marks B, Zielinski T, Yueh MF, Raucy J. A simultaneous assessment of CYP3A4 metabolism and induction in the DPX-2 cell line. AAPS J 2005;7:E6–13.
[63] Crouthamel MH, Wu D, Yang Z, Ho RJ. A novel MDR1 G1199T variant alters drug resistance and efflux transport activity of P-glycoprotein in recombinant Hek cells. J Pharm Sci 2006;95:2767–77.